ARTICLE

Check for updates

N^6-methyladenosine modification of the *Aedes aegypti* transcriptome and its alteration upon dengue virus infection in Aag2 cell line

Zhenkai Dai[1], Kayvan Etebari [1] & Sassan Asgari [1]✉

The N^6-methyladenosine (m^{6}A) modification of RNA has been reported to affect viral infections. Studies have confirmed the role of m^{6}A in replication of several vector-borne flaviviruses, including dengue virus (DENV), in mammalian cells. Here, we explored the role of m^{6}A in DENV replication in the mosquito *Aedes aegypti* Aag2 cell line. We first determined the presence of m^{6}A on the RNAs from mosquito cells and using methylated RNA immunoprecipitation and sequencing (MeRIP-Seq) identified m^{6}A modification of the mosquito transcriptome and those that changed upon DENV infection. Depletion of m^{6}A methyltransferases and the m^{6}A binding protein YTHDF3 RNAs decreased the replication of DENV. In particular, we found that the *Ae. aegypti ubiquitin carrier protein 9* (*Ubc9*) is m^{6}A modified and its expression increases after DENV infection. Silencing of the gene and ectopic expression of Ubc9 led to reduced and increased DENV replication, respectively. The abundance of *Ubc9* mRNA and its stability were reduced with the inhibition of m^{6}A modification, implying that m^{6}A modification of *Ubc9* might enhance expression of the gene. We also show that the genome of DENV is m^{6}A modified at five sites in mosquito cells. Altogether, this work reveals the involvement of m^{6}A modification in *Ae. aegypti*-DENV interaction.

[1] Australian Infectious Disease Research Centre, School of Biological Sciences, The University of Queensland, Brisbane, Queensland, Australia.
✉email: s.asgari@uq.edu.au

Nucleotides in RNA molecules are known to be modified by more than 100 different modifications, however, N[6]-methyladenosine (m[6]A) is the most common RNA modification, particularly in mRNAs and long non-coding RNAs[1,2]. m[6]A affects almost all aspects of mRNA metabolism, including splicing, translation, stability and maturation[3–5]. Recent findings have indicated that m[6]A methylation is not static, but a dynamic and reversible modification in RNA[2,6]. There are three sets of proteins involved in dynamic m[6]A modification: writers, readers, and erasers. m[6]A writers are responsible for RNA methylation and form a multiprotein complex consisting of methyltransferase-like 3 (METTL3), METTL14, and Wilms' tumour 1-associated protein (WTAP), in which METTL3 has a catalytic function, METTL14 has an RNA-binding property, and WTAP is a stabilizing factor[7]. The METTL3-METTL14-WTAP complex targets the consensus motif DRACH (where D = G/A/U, R = G/A and H = U/A/C) in mRNAs[8–10]. m[6]A modification can be removed by m[6]A erasers or demethylases such as fat mass and obesity-associated protein (FTO) and ALKB homologue 5 (ALKBH5) protein[11,12]. Finally, m[6]A readers, that specifically bind to m[6]A, mediate m[6]A modification functions that range from blocking or inducing protein-RNA interactions or facilitating subsequent reactions such as alternative splicing, promoting translation of m[6]A-modified mRNA or targeting mRNA for degradation[2]. The major m[6]A readers in the nucleus are heterogeneous nuclear ribonucleoprotein C (HNRNPC) and HNRNPA2B1, and in the cytoplasm, YTH-domain family 1 (YTHDF1) and YTHDF2 proteins[13,14].

m[6]A analysis is a relatively new area of research and the relevant literature on insects is currently scant and almost non-existent on mosquitoes; except one, in which m[6]A modification of mRNAs in *Aedes albopictus* was shown in 1977 using a biochemical approach[15]. More recently, m[6]A RNA modification was shown in *Drosophila melanogaster* and its role in neural function and sex determination was established[3]. Further, m[6]A has also been shown in the silkworm, *Bombyx mori*. Knocking down *BmMETTL3* and *BmMETTL14* in a *B. mori* cell line resulted in the arrest of cell cycle progression and deficiency of chromosome alignment and segregation[16].

Aedes aegypti is the most common epidemic mosquito vector in tropical and subtropical regions transmitting a variety of viruses such as dengue virus (DENV), Zika virus (ZIKV), Yellow fever virus, and Chikungunya virus. DENV, a single-stranded positive-sense RNA virus from the viral family *Flaviviridae*[17], alone is responsible for nearly 400 million annual cases of DENV infectious diseases, including half a million of dengue haemorrhagic fever, from more than 100 countries[18,19]. In mosquitoes, DENV replicates but does not undermine the vector's survival, which is realized by inhibiting the vector's immunity to the extent that only allows it to multiply to a non-pathogenic level[20,21]. This entails an optimal balancing between viral replication and host anti-viral responses regulated by the host genes.

Many flaviviruses have m[6]A modification on their RNA in infected mammalian cells. ZIKV RNA is rich in m[6]A modification sites[22,23], and its replication has been proved to be regulated by methyltransferases METTL3 and METTL14 as well as demethylases ALKBH5 and FTO in human cells. It has been demonstrated that m[6]A can regulate Hepatitis C virus (HCV) infection[22]. Furthermore, researchers analysed the effect of the reading protein YTHDF1-3 on ZIKV replication and found that silencing the m[6]A binding protein, YTHDF2, caused the greatest increase in ZIKV replication[23]. The possible explanation is that YTHDF2 may inhibit the replication of ZIKV by binding to the viral RNA and destabilizing it[23]. Gokhale et al. found that interfering with m[6]A methyltransferases or m[6]A demethylases, respectively, increases or decreases the replication of HCV. During HCV infection, the host cell's YTHDF protein re-localized to lipid droplets, which are the

sites of virus assembly, indicating that YTHDF is able to bind to the virus[22]. The authors also produced mutation of the m[6]A modification site on the *E1* gene of HCV, and the result demonstrated increased binding of viral RNA to the nucleocapsid protein (or core protein) and decreased viral RNA binding to the YTHDF protein, which further led to an increase in infectious virus particles. Gokhale et al., hence, speculated that YTHDF proteins may inhibit the production of infectious virions by competing with nucleocapsid proteins for viral RNA[22].

In this study, we aimed to investigate the role of m[6]A in DENV replication in the mosquito *Ae. aegypti* by using the Aag2 cell line. Our results suggest that DENV infection indeed leads to changes in m[6]A on mosquito transcripts. We demonstrate that the replication of DENV is positively regulated by the m[6]A methyltransferases and m[6]A binding protein, a YTH family protein. We also identified m[6]A modified sites across the DENV RNA genome. Further, we investigated the role of the highly induced *SUMO-conjugating enzyme Ubc9-B* gene with m[6]A modification in DENV replication. Together, our results shed further light on DENV-mosquito interaction and the role m[6]A modification of host and viral genomic RNA play in the interaction.

Results

Identification of RNA m[6]A methylation in *Ae. aegypti*. To find out if m[6]A on RNAs occurs in *Ae. aegypti*, first we performed a dot blot assay by using a commercial monoclonal antibody against m[6]A in an RNA sample isolated from cultured mosquito Aag2 cells. RNA from Vero cells (kidney epithelial cells extracted from an African green monkey) and in vitro synthesized *Enhanced green fluorescent protein* (EGFP) transcripts were used as positive and negative controls, respectively. As shown in Fig. 1b, there are strong m[6]A signals in RNAs from both Aag2 and Vero cells, but not in the *EGFP* transcripts, indicating that the RNAs from *Ae. aegypti* contain m[6]A modification.

To determine the m[6]A landscape and identify detailed m[6]A sites on the *Ae. aegypti* transcripts, we performed methylated RNA immunoprecipitation and sequencing (MeRIP-Seq) on *Ae. aegypti* Aag2 cells (Fig. 1a). Normalized density of m[6]A peaks between immunoprecipitated (IP) and input samples indicated enrichment of m[6]A in the IP samples (Fig. 1c). Following calling peaks in IP over input samples and after all filtering steps, a total of 4410 peaks were identified (Supplementary Data 1).

We then further explored the m[6]A distribution profiles to understand the topological pattern of m[6]A methylation in the mosquito transcriptome. We found that m[6]A peaks were abundant in the coding regions (39%), followed by 20% in the intergenic regions, 18% in the 5′UTR, 17% in introns, and 6% in the 3′ UTRs (Fig. 1d). A snapshot of m[6]A enriched regions on the three chromosomes of *Ae. aegypti* and three representative genes with m[6]A peaks are shown in Supplementary Figs. 1 and 2, respectively. The analysis of m[6]A sequence preference identified AAACU as the most frequent motif (Fig. 1e), showing consistency with the known m[6]A motif DRACH[8–10]. In total, there were 2073 genes identified with m[6]A peaks (some genes have more than one peak).

Functional annotation of m[6]A modified transcripts from *Ae. aegypti*. To explore what sort of transcripts are modified by m[6]A in *Ae. aegypti*, we first classified the genes into Gene Ontology (GO) terms. The analysis identified 2502, 903, and 465 GO terms in biological process, molecular function, and cellular components, respectively (Supplementary Data 2). In biological processes category, cellular process, and metabolic process were the top two enriched terms (Supplementary Fig. 3). In molecular function, GO terms associated with "binding" were significantly
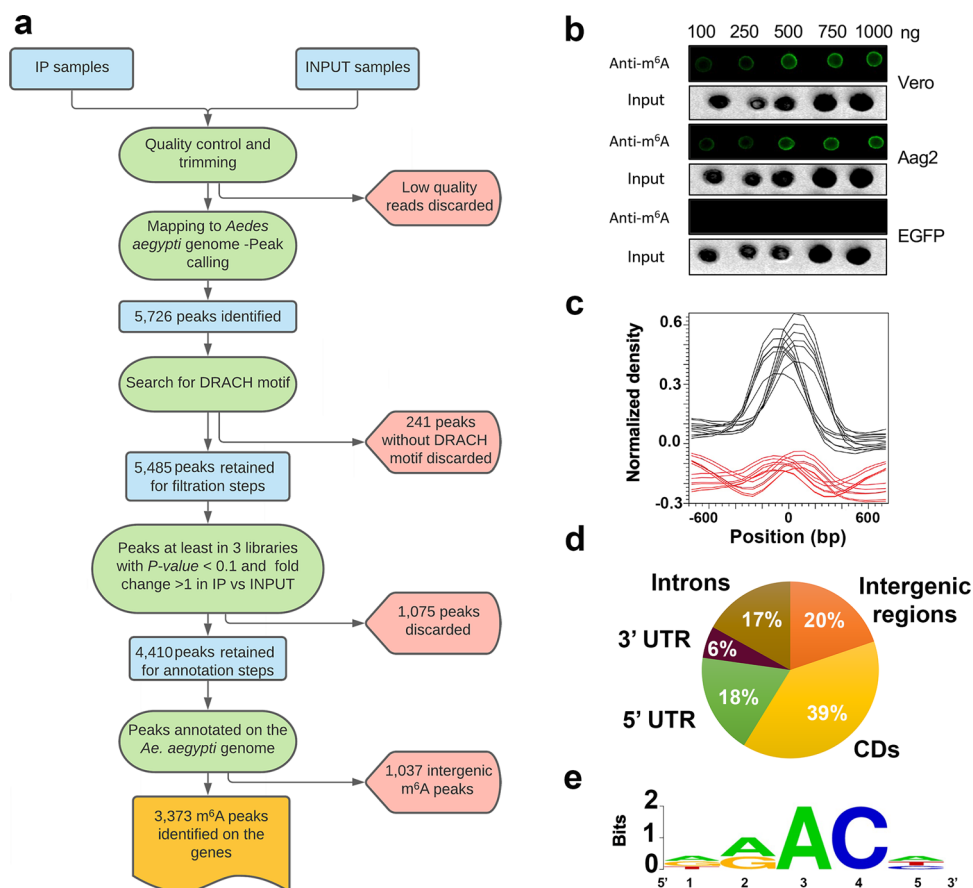
Fig. 1 m6A modification of *Ae. aegypti* transcripts analysed by dot blot and methylated RNA immunoprecipitation and sequencing (MeRIP-Seq). a A diagram showing the MeRIP-Seq data analysis procedure. **b** Confirmation of RNA N6-methyladenosine (m6A) methylation in *Ae. aegypti*. Total RNA from Aag2 and Vero cells were extracted and subjected to a dot blot assay using a specific anti-m6A antibody. EGFP transcripts were synthesised in vitro and used as negative control. The input RNAs were directly stained with ethidium bromide. **c** Normalized density of m6A peaks between immunoprecipitated (black lines) and input (red lines) samples following MeRIP-Seq indicating enrichment of m6A in the IP samples as part of the quality control of the data. **d** Pie chart showing distribution of m6A peaks in *Ae. aegypti* transcripts regions. **e** The consensus m6A motif DRA*CH (D = G/A/U, R = G/A, * modified A, H = U/A/C) was enriched in the identified m6A peaks.

enriched, and GO terms related to catalytic and hydrolase activity were among highly enriched GO terms. In cellular components category, cellular anatomical entity, intercellular anatomical structure, organelle, ribonucleoprotein complex were among the terms enriched (Supplementary Fig. 3, Supplementary Data 2). The scatterplots generated based on the enriched GO terms in Revigo provide an overview of the most abundant terms in each category (Fig. 2).

DENV infection changes the m6A modification of *Ae. aegypti* cellular transcripts. To find out whether m6A modification alters following infection of mosquito cells with DENV, we compared the m6A profile in DENV-infected Aag2 cells (5 days post-infection) with that in uninfected cells by analysing data from MeRIP-Seq. DENV infection was confirmed in the infected samples prior to MeRIP-Seq (Fig. 3a). We identified 147 genes that showed modified m6A peaks when mock and DENV-infected samples were compared (Fig. 3b; Supplementary Data 3). Subsequently, we compared the mock and DENV-infected input groups and identified 319 significantly differentially expressed genes (DEGs) after virus infection (Fig. 3b, c; Supplementary Data 4). Of those, 26 genes were found to have m6A peaks (Table 1; Fig. 3b, c, blue and red dots). Among these DEGs, there were 176 up-regulated and 143 down-regulated genes, which, respectively, included 10 and 16 genes modified with m6A (Fig. 3c–e; Table 1). Of those, m6A peaks

of nine genes increased and 17 decreased, however, only four genes showed significantly modified m6A peak that were also significantly differentially expressed (Fig. 3c; Table 1). The results confirmed that DENV infection did cause changes to m6A modification in mosquito cells.

m6A machinery is involved in DENV replication in *Ae. aegypti*. To find out if overall m6A modification has any effect on DENV replication in mosquito Aag2 cells, we used 3-Deazaadenosine (3-DAA; concentration from 0 to 300 μM), a known m6A inhibitor[24]. Dot blot results showed 3-DAA could effectively reduce the m6A levels of total RNA in Aag2 cells (Fig. 4a). Subsequently, we infected 3-DAA-treated Aag2 cells with 1 MOI DENV. RT-qPCR was performed at 72 hpi. Treatment of cells with 3-DAA significantly decreased ($p = 0.028$) the levels of DENV genomic RNAs (Fig. 4b). Therefore, the results suggest that m6A positively regulates the replication of DENV in mosquito cells. Of note, 3-DAA treatment of Aag2 cells had no effect ($p = 0.279$) on cell survival (Fig. 4c).

The homologous genes of the RNA methyltransferases *METTL3* and *METTL14* were blasted against the *Ae. aegypti* genome based on the reported human sequences. We compared the MTA-70 domains from METTL3 and METTL14 between *Homo sapiens* and *Ae. aegypti*. The multiple sequence alignments showed highly conserved domains of MTA-70 between METTL3
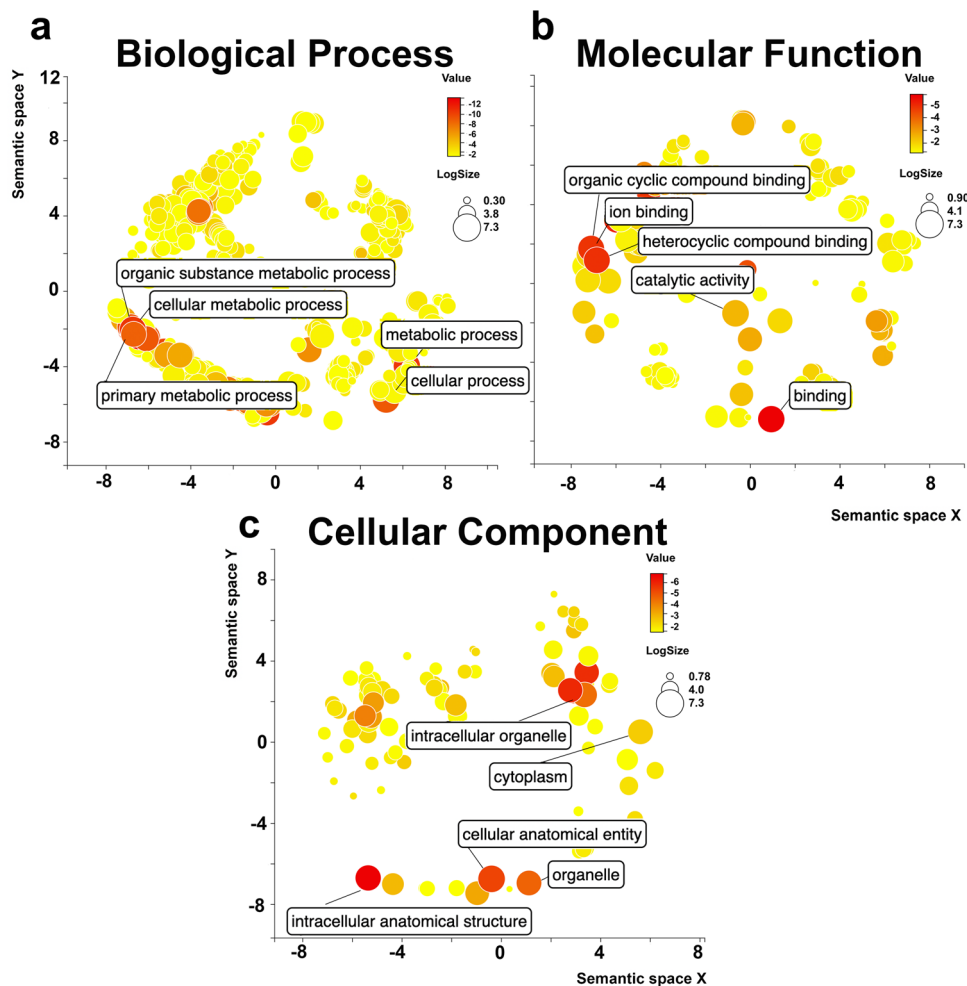
Fig. 2 Gene ontology scatterplot of *Ae. aegypti* transcripts with m6A modification. The scatterplot shows the cluster representatives of GO terms identified from *Ae. aegypti* transcripts with m6A modification generated by Revigo. These GO terms remained after the redundancy reduction, in a two-dimensional space derived by applying multi-dimensional scaling to a matrix of the GO terms' semantic similarities. **a** Biological process, **b** molecular function and **c** cellular component.

and METTL14 proteins from the mosquito and human (Supplementary Fig. 4a). In addition, a homologous gene of the reader *YTHDF3* was found in the *Ae. aegypti* genome. Alignment of YTHDF3 proteins between *Ae. aegypti* and *H. sapiens* showed a low overall degree of protein conservation. However, multiple amino acid sequence alignment showed a highly conserved YTH domain (Supplementary Fig. 4b) between *Ae. aegypti* and *H. sapiens*. Then, we compared these three sequences from eight species to analyse their homologies and established phylogenetic trees by using MEGA5 software with the neighbour-joining method. Accordingly, all the invertebrates (*Drosophila melanogaster*, *Bombyx mori* and *Ae. aegypti*) clustered together and separated from the vertebrate gene sequences (Supplementary Fig. 5a–c).

To further determine whether m6A modification affects DENV replication, we knocked down the m6A methyltransferases, *METTL3* and *METTL14*, in Aag2 cells through RNAi and infected the cells with DENV. RT-qPCR was performed on RNA extracted from cells collected at 72 h post infection (hpi), which confirmed effective silencing of *METTL3* (75%) and *METTL14* (85%) (Fig. 5a, b). *METTL3* and *METTL14* depletion significantly decreased (~2.5-4-fold; $p < 0.0001$) the levels of DENV genomic RNA (gRNA; Fig. 5c). Silencing of *METTL3* and *METTL14* together also led to declined DENV gRNA levels but to the same extent as single gene silencing (Fig. 5c). *METTL3* and *METTL14*

depletion, separately or together, also decreased ($p < 0.0001$) the titre of DENV determined by plaque assay (Fig. 5d). These results suggested a positive correlation between the m6A writers and DENV replication.

As for the effect of m6A reader on DENV replication, we knocked down *YTHDF3* by using dsRNA to the gene (Fig. 6a). RT-qPCR analysis was performed at 72 hpi. Figure 6b shows that *YTHDF3* depletion significantly reduced ($p < 0.001$) the levels of DENV gRNA. Also, *YTHDF3* depletion led to decreased ($p < 0.005$) titre of DENV (Fig. 6c).

***Ubc9* is m6A modified and facilitates replication of DENV**. We selected four most significantly DEGs (AAEL026586, AAEL011112, AAEL020023, AAEL025779, coding, respectively, for an unspecified protein, alcohol dehydrogenase, histone H2B, and Ubc9; Supplementary Data 4) and explored their potential influence on DENV replication. Two of these genes (AAEL026586 and AAEL025779) were m6A modified and two were not (AAEL011112 and AAEL020023). As these DEGs genes were all up-regulated, we, respectively, knocked them down in Aag2 cells (Fig. 7a) and then infected them with DENV-2 at MOI of 1. The results indicated that depletion of AAEL025779 gene reduced DENV replication ($p = 0.0007$), but depletion of the other three genes did not bring significant changes to DENV
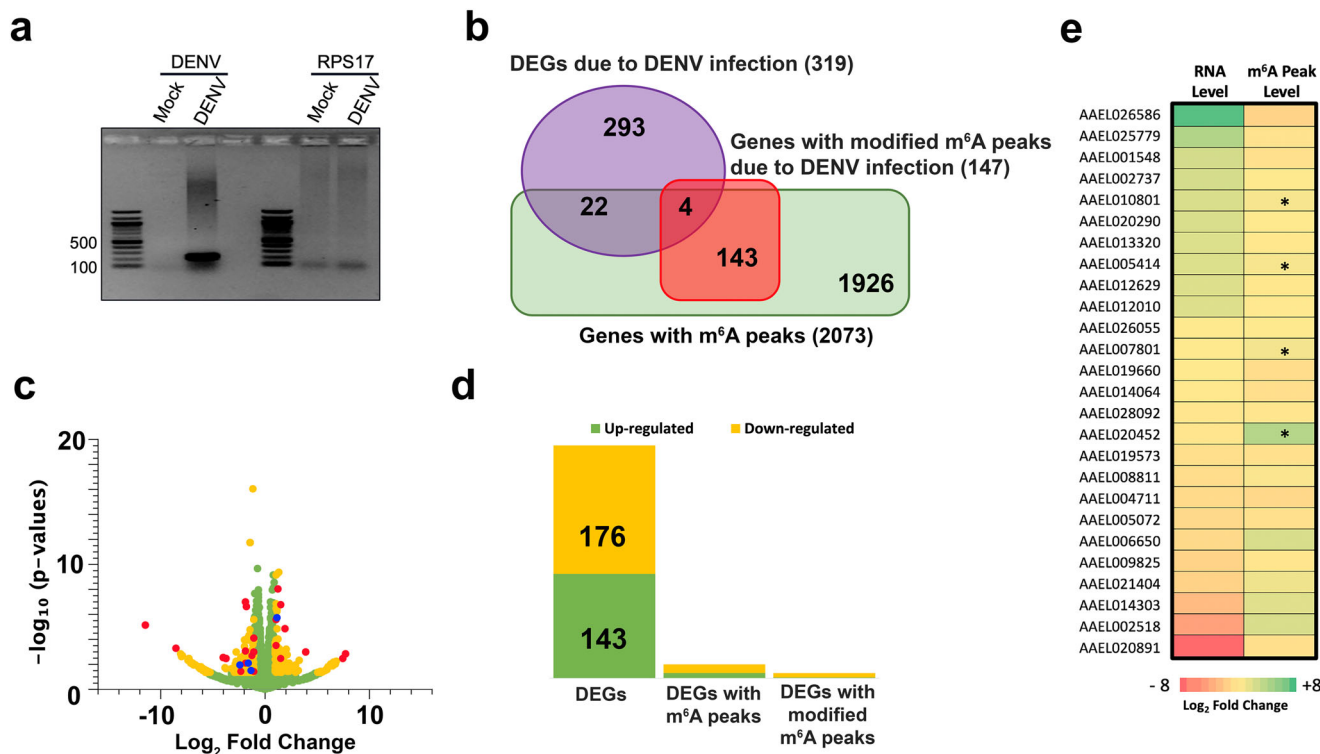
Fig. 3 Dengue virus infection alters m⁶A modification of *Ae. aegypti* transcripts. a Confirmation of DENV infection of Aag2 cells. RT-PCR analysis of RNA extracted from Aag2 (Mock) and Aag2 cells infected with 1 MOI DENV 5 days after infection using DENV-specific and RPS17 (control) primers. The PCR products were analysed on an agarose gel. **b** Venn diagram showing summarized numbers of differentially expressed genes, with and without m⁶A peak changes. **c** Volcano plot showing differentially expressed genes in Aag2 cells in response to DENV infection. Green and yellow dots represent up-regulated and down-regulated genes with fold change >2 and *p* value <0.05, and those in red and blue are DEGs with m⁶A peaks, with the blue ones being DEGs with changed m⁶A peaks upon DENV infection. **d** Number of significantly differentially expressed genes between mock and DENV-infected Aag2 cells at five days post infection among which there were 26 with m⁶A peaks, of which four showed modified m⁶A upon DENV infection. **e** Heatmap of *Ae. aegypti* genes with m⁶A sites, which were differentially expressed in response to DENV infection (see Table 1 for the list of genes). The four genes that showed differential m⁶A and gene expression upon DENV infection are indicated by asterisks.

replication (Fig. 7b). AAEL025779 encodes the SUMO-conjugating enzyme Ubc9, an important enzyme in the SUMOylation pathway, and was found to be m⁶A modified at the 3′UTR (Fig. 7c). Up-regulation of *Ubc9* was also confirmed by RT-qPCR in Aag2 cells infected with DENV for 72 h, consistent with the RNA-Seq data (Fig. 7d).

Subsequently, we constructed a plasmid, pSLfa-Ubc9-GFP, to overexpress *Ubc9* in fusion with *GFP* in Aag2 cells and then infected the cells with DENV-2 at MOI of 1. The results showed that the overexpression of Ubc9 led to increased replication of DENV (Fig. 7e). Overall, the results suggest that Ubc9 facilitates the replication of DENV.

Inhibition of m⁶A modification decreases the transcript levels of *Ubc9*. In order to explore the role of m⁶A modification in *Ubc9* expression, we knocked down the m⁶A methyltransferases, *METTL3* and *METTL14*, separately through RNAi and infected the cells with DENV. RT-qPCR was performed at 72 h post infection (hpi). Figure 8a shows that the dsRNA of *METTL3* and *METTL14* reduced the transcript levels of the two m⁶A methyltransferases by about 50% and 40%, respectively. While depletion of *METTL14* significantly decreased the levels of *Ubc9* RNAs ($p < 0.0001$), depletion of *METTL3* did not lead to a statistically significant reduction of *Ubc9* transcript levels (Fig. 8b). In addition, we inhibited m⁶A modification in Aag2 cells by using the known m⁶A inhibitor, 3-DAA. As a result, the transcript levels of *Ubc9* significantly decreased (Fig. 8c; $p = 0.0233$). Taken these

results, we found that the expression of *Ubc9* could be regulated by m⁶A modification.

m⁶A modification affects the mRNA stability of *Ubc9*. m⁶A can alter mRNA metabolism, including splicing, translation, and stability to affect gene expression[2]. For the specific gene *Ubc9*, we took a closer look at its mRNA stability, and explored whether m⁶A modification affects the expression of *Ubc9* through regulating its mRNA stability. We used Actinomycin D, an inhibitor of transcription, to assess the mRNA stability of *Ubc9* during DENV infection and found that upon DENV infection the stability of *Ubc9* mRNA increased (Fig. 9a). In addition, 3-DAA was used to inhibit m⁶A modification in DENV-infected Aag2 cells, and then the *Ubc9* mRNA stability was assessed (Fig. 9b). The results showed that inhibiting m⁶A methylation decreased the mRNA stability of *Ubc9*.

m⁶A methylation in DENV RNA. It has been reported that DENV genomes contain m⁶A modification in infected mammalian cells[22]. We hypothesized that the DENV gRNA is also modified by m⁶A during infection in infected mosquito cells. To confirm this, we carried out MeRIP-RT-qPCR on total RNA harvested from DENV-infected Aag2 cells collected at 72 hpi. This involved m⁶A RNA enrichment followed by RT-qPCR using primers to the DENV genome. DENV RNA was specifically enriched by the anti-m⁶A antibody, but not by IgG (Fig. 10a). This enrichment was found in DENV RNA from both

Table 1 The list of *Aedes aegypti* genes with m⁶A sites, which were differentially expressed in response to DENV infection.

Name	Gene description	Fold change	p-value	DENV-infected (RPKM)	Mock (RPKM)	m⁶A Peak
AAEL026586	Unspecified product	179.5	3.57E-03	0.090	0.000	Peaks 1170, 1171, 1172, 1173, 1174, 1175
AAEL025779	SUMO-conjugating enzyme UBC9-B	10.01	5.28E-03	0.100	0.010	Peak 5676
AAEL001548	Glucosyl/glucuronosyl transferases	2.97	3.88E-03	0.180	0.070	Peak 75
AAEL002737	Cytochrome c oxidase, subunit VIIC, putative	2.92	1.84E-07	2.450	1.090	Peak 419
AAEL010801	*Cytochrome b-c1 complex subunit 6*	2.52	4.63E-07	3.780	1.960	Peak 2602
AAEL020290	60S ribosomal protein L39	2.46	9.30E-09	21.180	11.470	Peak 3632
AAEL013320	Translocon-associated protein, delta subunit	2.21	2.07E-06	2.830	1.760	Peak 2056
AAEL005414	*ER membrane protein complex subunit 6*	2.19	1.49E-07	3.780	2.260	Peak 5123
AAEL012629	Deoxyuridine 5'-triphosphate nucleotidohydrolase	2.11	3.23E-04	1.270	0.780	Peak 1207
AAEL012010	Conserved hypothetical protein	2.1	2.62E-06	1.770	1.100	Peak 3237
AAEL026055	Unspecified product	-2	0.04	0.070	0.180	Peaks 893, 894, 895
AAEL007801	*Exonuclease*	-2.03	9.21E-05	0.530	1.440	Peak 2577
AAEL019660	Zwei Ig domain protein zig-8-like isoform X2	-2.07	1.15E-03	0.070	0.170	Peaks 2648, 2649, 2650
AAEL014064	Glutaredoxin, putative	-2.1	2.62E-06	12.950	35.310	Peak 1640
AAEL028092	Fibroblast growth factor receptor homologue 1	-2.27	2.35E-03	0.060	0.180	Peak 5095
AAEL020452	*Titin-like protein*	-2.44	4.00E-02	0.005	0.020	Peaks 249, 250
AAEL019573	Hemicentin-1	-3.02	8.11E-03	0.020	0.070	Peak 2187
AAEL008811	NADH dehydrogenase 3	-3.36	2.77E-07	2.320	10.690	Peak 5723
AAEL004711	Testis specific leucine rich repeat protein	-3.64	8.32E-03	0.040	0.190	Peak 1555
AAEL005072	MRAS2, putative	-3.84	0.02	0.020	0.080	Peak 5390
AAEL006650	Potassium channel beta	-3.9	6.93E-03	0.009	0.050	Peak 2792
AAEL009825	60S ribosomal protein L13a	-4.83	4.00E-02	0.030	0.210	Peak 5624
AAEL021404	Unspecified product	-5.02	1.00E-02	0.010	0.090	Peak 5605
AAEL014303	Neuroligin	-12.64	3.78E-03	0.002	0.030	Peak 936
AAEL002518	Glutamate receptor, ionotropic kainate 1, 2, 3	-37.12	0.05	0.000	0.010	Peak 4351
AAEL020891	Vacuolar protein sorting-associated protein 13B	-359.05	5.54E-04	0.000	0.080	Peak 5667

Only four genes (in italic) showed differential m⁶A and gene expression upon DENV infection.

intracellular as well as extracellular fractions, suggesting that the released virions most likely also contain m⁶A modified gRNA.

We next mapped the sites of the DENV RNA genome modified by m⁶A using the MeRIP-Seq data. We identified five m⁶A peaks in DENV gRNA (Fig. 10b and Supplementary Table 1). This further confirmed that DENV gRNA is modified by m⁶A in infected mosquito cells. Two m⁶A peaks were found on the NS5 coding region and one peak each on the pM, NS1-NS2A and NS4B-NS5 coding regions. DENV pM and NS1 facilitate the formation and maturation of the viral particles. NS2A and NS4B are involved in DENV virion assembly. NS5 contains a methyltransferase and a polymerase domain, which are essential for the replication of the DENV RNA genome.

Discussion

In this study, we demonstrated m⁶A modification of *Ae. aegypti* RNAs and further determined the global landscape of m⁶A modifications on the mosquito transcriptome through MeRIP-Seq. In total, we identified 4410 m⁶A-related peaks that were mostly in the coding region followed by the intergenic regions. Analysis of the sequencing results shed light on the function of the m⁶A modified transcripts. These were classified in the three GO categories of biological processes, molecular functions, and cellular components, with most of them found in biological processes.

Previous studies have demonstrated alterations in the m⁶A profile of mammalian cells upon virus infection[22,23,25,26]. Relevant to this study, several viruses from *Flaviviridae* (DENV, ZIKV, WNV and HCV) were shown to change the landscape of m⁶A on the transcriptome of human Huh7 cells[27]. Further, ZIKV infection led to changes in m⁶A modification of transcripts in human embryonic kidney 293T cells[23]. Gokhale et al. discovered that DENV infection changed the m⁶A modification of *RIOK3* and *CIRBP* genes, through interferon-β (IFN) and the endoplasmic reticulum stress pathway. They further demonstrated that the alteration of the m⁶A modification on RIOK3 and CIRBP can, in return, enhance DENV replication in human cells[27]. Given this, it is possible that DENV utilizes these pathways to change the expression of the host pro-viral and anti-viral genes (*RIOK3* and *CIRBP*) and as a result benefit its replication[27]. However, we did not find any changes either in the expression of the *RIOK3* and *CIRBP* genes or in their m⁶A modification in mosquito Aag2 cells. In addition, we sought out the human genes showing significant m⁶A peak changes upon DENV infection from Gokhale et al. and found their homologues in the *Ae. aegypti* genome to see if any of them show changes in m⁶A during DENV infection[27]. Yet none of them, including the homologues of *RIOK3* and *CIRBP*, showed m⁶A changes. This suggests that DENV infection may have different effects on m⁶A modification between humans and mosquitoes. It is known that DENV presents different pathogenicities in the mosquito vector and the human host and this could be reflected in differences in m⁶A modifications in the host and the vector. In the mosquito vector, DENV presents rather a persistent infection, whereas the virus infection can be acute in humans[28,29].

The m⁶A machinery functions through the regulation of three groups of enzymic proteins in host cells, including the m⁶A writers, readers, and erasers[7]. A large body of research evidence has confirmed that depletion of these proteins affects viral replication. Interfering with the expression of the m⁶A reader, YTHDF1-3, enhanced the production of ZIKV and HCV through reducing the binding of the reader to the viral genomes where m⁶A modifications occur[22,23]. In addition, some host RNAs which contain m⁶A sites have been reported to affect viral replication. For example, methylation of oxoglutarate
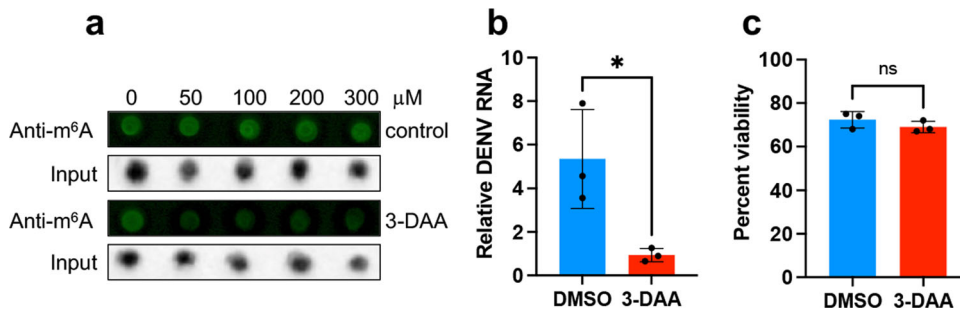
Fig. 4 3-Deazaadenosine, an inhibitor of m6A, reduces DENV replication in *Ae. aegypti* cells. a Confirmation of the effect of 3-DAA on inhibition of m6A modification in Aag2 cells. Total RNA from 3-DAA treated Aag2 and control cells (DMSO treated) were extracted and subjected to a dot blot assay using a specific anti-m6A antibody. The input RNAs were directly stained with ethidium bromide. **b** Inhibition of DENV replication by 3-DAA. Aag2 cells treated with 100 μM 3-DAA or DMSO were infected with DENV 72 h after treatment with 3-DAA. Cells were collected at 72 hpi for quantification of DENV RNA by RT-qPCR. **c** Viability of Aag2 cells treated with 3-DAA (100 μM) measured at 72 hpi. Error bars represent mean ± S.D. ns, not significant; *$p < 0.05$, t-test.
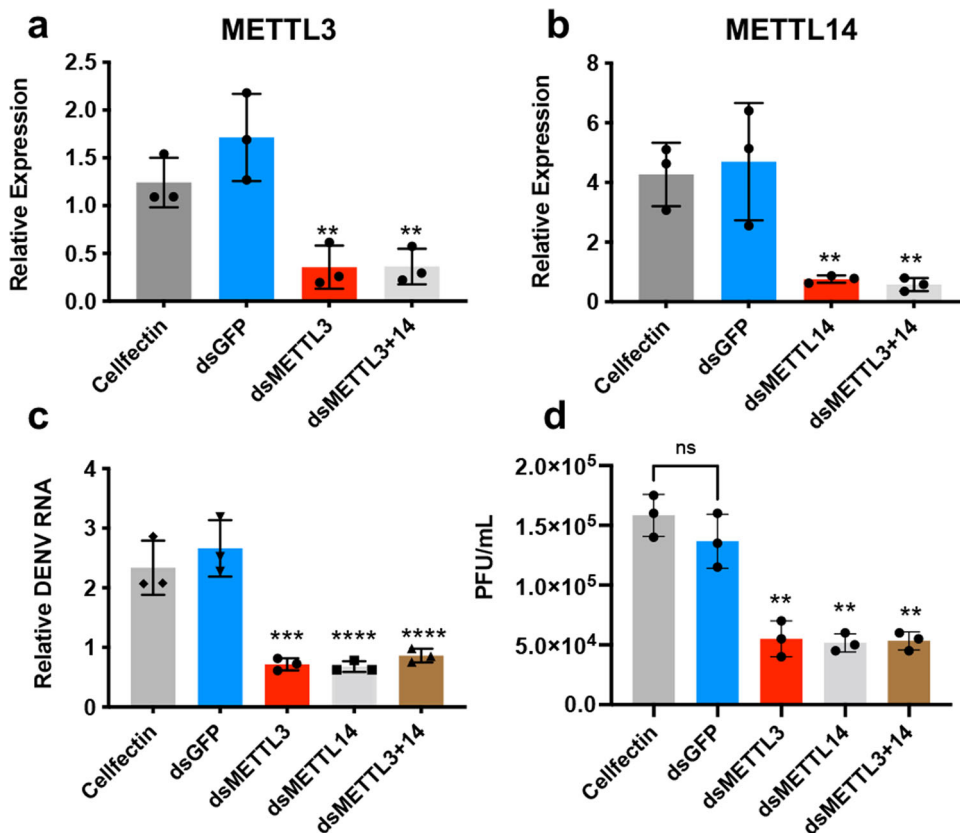
Fig. 5 Silencing m6A methyltransferase genes reduces DENV replication. Expression levels of **a** *METTL3* and **b** *METTL14* in Aag2 cells transfected with dsRNA to *METTL3* (dsMETTL3), and double transfection with dsRNAs to *METTL3* and *METTL14*. dsRNA to *GFP* (dsGFP) was used as negative control in addition to the Cellfectin transfection reagent only. **c**, **d** Reductions in DENV replication in Aag2 cells by silencing *METTL3/METTL14* or both. Cells were collected at 72 hpi for RNA extraction and quantification of DENV RNA by RT-qPCR (**c**), and the supernatants were harvested for quantification of DENV virions by plaque assay (**d**). Error bars represent mean ± S.D. ns, not significant, **$p < 0.01$; ***$p < 0.001$; ****$p < 0.0001$. ANOVA test with post hoc comparisons.

dehydrogenase (OGDH) mRNA was shown to decrease the replication of Vesicular stomatitis virus (VSV). The outcome provided a novel strategy for researchers to develop a drug targeting the methylation of OGDH mRNA for the control of VSV infection[25]. In DENV infection, we found the mosquito m6A writer METTL3, METTL14 and m6A reader YTH family protein affect DENV replication. Silencing of these genes through RNAi led to reduced DENV replication suggesting that unlike in human cells, m6A machinery facilitates DENV replication. However, the off-target effects of these RNAi experiments done in previous works and this study cannot be ruled out.

m6A modification on viral genomic RNA can affect viral infection. The m6A sites on the envelope gene of HCV and ZIKV have been confirmed to facilitate suppression of viral replication through binding with the reader, YTHDF protein[22,23]. In the 3′ UTR of DENV, there are two stem-loops whose function is to control viral transmission from mosquito to human[30]. Of note, while we did not find any m6A peak in DENV 3′UTR replicated in mosquito cells, one peak was detected in this region (10273-10300) on the DENV genome when replicated in mammalian cells[22]. As such, the m6A modification on the 3′UTR may be related to the vector-borne transmission mechanism[31]. We found
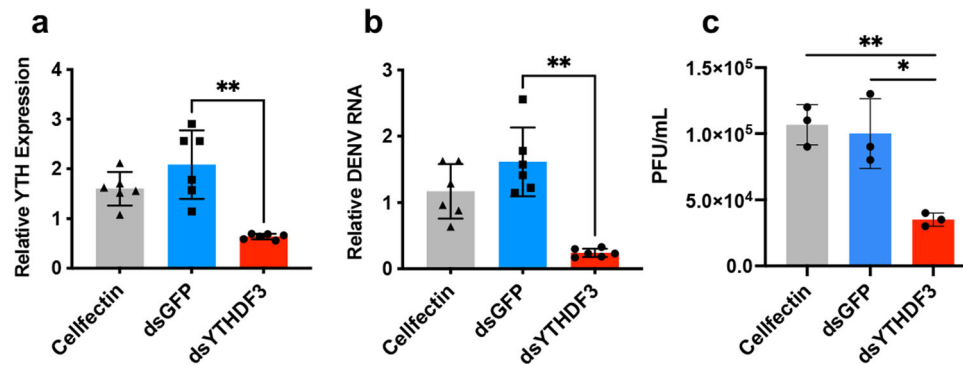
Fig. 6 m6A YTHDF3 reader modulates DENV replication in *Ae. aegypti* cells. a Confirmation of silencing of *YTHDF3* homologue by dsRNA (dsYTHDF3) in Aag2 cells. dsRNA to *GFP* (dsGFP) was used as a negative control in addition to Cellfectin transfection reagent only. **b, c** Inhibition of DENV replication by *YTHDF3* silencing. Aag2 cells transfected with dsRNA targeting *GFP* or dsRNA targeting *YTHDF3* were infected with DENV 72 h after transfection. Cells were collected at 72 hpi for RNA extraction and quantification of DENV RNA by RT-qPCR (**b**), and the supernatants were harvested for quantification of DENV virions by plaque assay (**c**). Error bars represent mean ± S.D. *$p < 0.05$; **$p < 0.01$. ANOVA test with post hoc comparisons.

that the genomic RNA of DENV contains m6A modification in precursor membrane (pM), non-structural protein 2A (NS2A), and non-structural protein 5 (NS5) coding regions when infecting mosquito cells. However, the function of m6A sites on the DENV RNA genome remains to be investigated. Gokhale et al. found DENV genome had prominent m6A sites in 11 sites in infected human Huh7 cells[27]. Of those, three peaks that were in the NS5 coding region have overlaps with those we found in the DENV genome replicated in Aag2 mosquito cells. This is a possible demonstration that some of the m6A modification sites on the viral genome may be conserved when DENV replicates in human and mosquito cells.

The present study identified 26 significantly DEGs with m6A peaks, some with m6A changes, when mock and DENV infected samples were compared. An altered gene *Ubc9*, which is m6A modified in mosquito cells, was found to facilitate DENV replication as its silencing led to reduced virus replication. Previous reports have indicated that several viruses may hijack the Ubc9 protein to support their infection[32–34]. Our results suggest that presumably DENV increases the transcript levels of *Ubc9* by increasing their stability mediated by m6A modification. The *Ubc9* gene encodes an important enzyme known as SUMO-conjugating enzyme Ubc9, which is involved in the SUMOylating pathway[35]. Small ubiquitin-like modifier (SUMO) proteins are involved in SUMOylation, a posttranslational modification process that is reversible and does not lead to protein degradation, unlike ubiquitination. SUMOylation affects various cellular processes, such as transcriptional regulation, apoptosis, protein stability, nuclear-cytosolic transport, cell cycle and virus infection[36]. Replication of a wide variety of viruses can be facilitated through impaired SUMOylating processes. Decreased SUMOylation of anti-viral proteins can interrupt anti-viral immune responses. On the other hand, some viruses may benefit from up-regulated SUMO proteins. For example, Influenza virus infection can cause a global increase in cellular SUMOylating and as a result enhanced replication of the virus[37]. The Ubc9 protein has been widely studied as a target of several viruses, including DENV, ZIKA, and HIV in mammalian cells. It has been shown that human Ubc9 protein can interact with HIV Gag protein and enhance replication of HIV[38]. In addition, Ubc9 has been reported to interact with DENV proteins, such as the DENV-2 envelope and NS5 proteins[39,40]. Silencing of *Ubc9* gene led to reduced DENV-2 replication in human Huh7 cells, consistent with our results in mosquito cells[40]. As such, we presume that the SUMOylation pathway may be involved in DENV infection in mosquitoes, in association with alteration in m6A modification.

In contrast, it was recently shown that depletion of core SUMOylation effector proteins, including Ubc9, in *Ae. aegypti* AF5 cells led to enhanced replication of ZIKV, Semliki Forest virus, and Bunyamwera virus[41].

There are only few studies that have established a link between m6A and SUMOylation with Ubc9 involvement. In human 293T cells, it was shown that METTL3 is SUMOylated and its SUMOylation reduces its m6A methyltransferase activity[42]. Further, in human liver cancer cell line MHCC97H, it was also found that METTL3 is SUMOylated by Ubc9, and increase in SUMOylation of METTL3 correlated with Ubc9 up-regulation[43]. Overall, up-regulation of *Ubc9* expression in mosquito Aag2 cells following DENV infection, through an increase in the stability of its mRNAs mediated by m6A modification, may lead to increases in SUMOylation, which is known to facilitate DENV replication in human cells[40]. However, establishing any direct link between m6A and SUMOylation in mosquito cells requires further investigations.

In summary, our results indicate that m6A RNA modification occurs in *Ae. aegypti*, and DENV infection alters the m6A repertoire of mosquito transcripts. The alteration of m6A caused by DENV in mosquitoes is, however, different from that found in human transcripts. Furthermore, we found the role of m6A machinery in positively affecting the replication of DENV. We also identified m6A modifications of the DENV genome. Furthermore, the transcript levels of a SUMOylation core protein, Ubc9, which is m6A modified, were found to increase with DENV infection. The results reveal that DENV may increase the stability of *Ubc9* transcripts ultimately supporting its own replication. The link and possible crosstalk between m6A modification and SUMOylation could be important in regulation of DENV replication, which deserves further exploration in future studies. This work contributes to our understanding of the differences of DENV m6A modification between human and *Ae. aegypti* infection, and the role of epigenetics in gene regulation during DENV infection in the mosquitoes.

Methods

Cells and viruses. *Ae. aegypti* Aag2 cells were cultured in 1:1 Mitsuhashi-Maramorosch and Schneider's insect medium (Invitrogen) supplemented with 10% foetal bovine serum (Bovogen Biologicals) at 28 °C. Vero cells were grown in Opti-MEM medium supplemented with 2% foetal bovine serum in a 37 °C incubator with CO_2. DENV serotype 2 East Timor strain (DENV-2 ET300) was used in infection experiments.

For virus infections, Aag2 cells were seeded in 6-well plates and allowed to attach for 1 h. Cells were then infected with 1 multiplicity of infection (1 MOI) of DENV-2 for 1 h at room temperature. Subsequently, fresh medium was added to cells and incubated at 28 °C. Duration of infections is indicated in the text or figure legends.
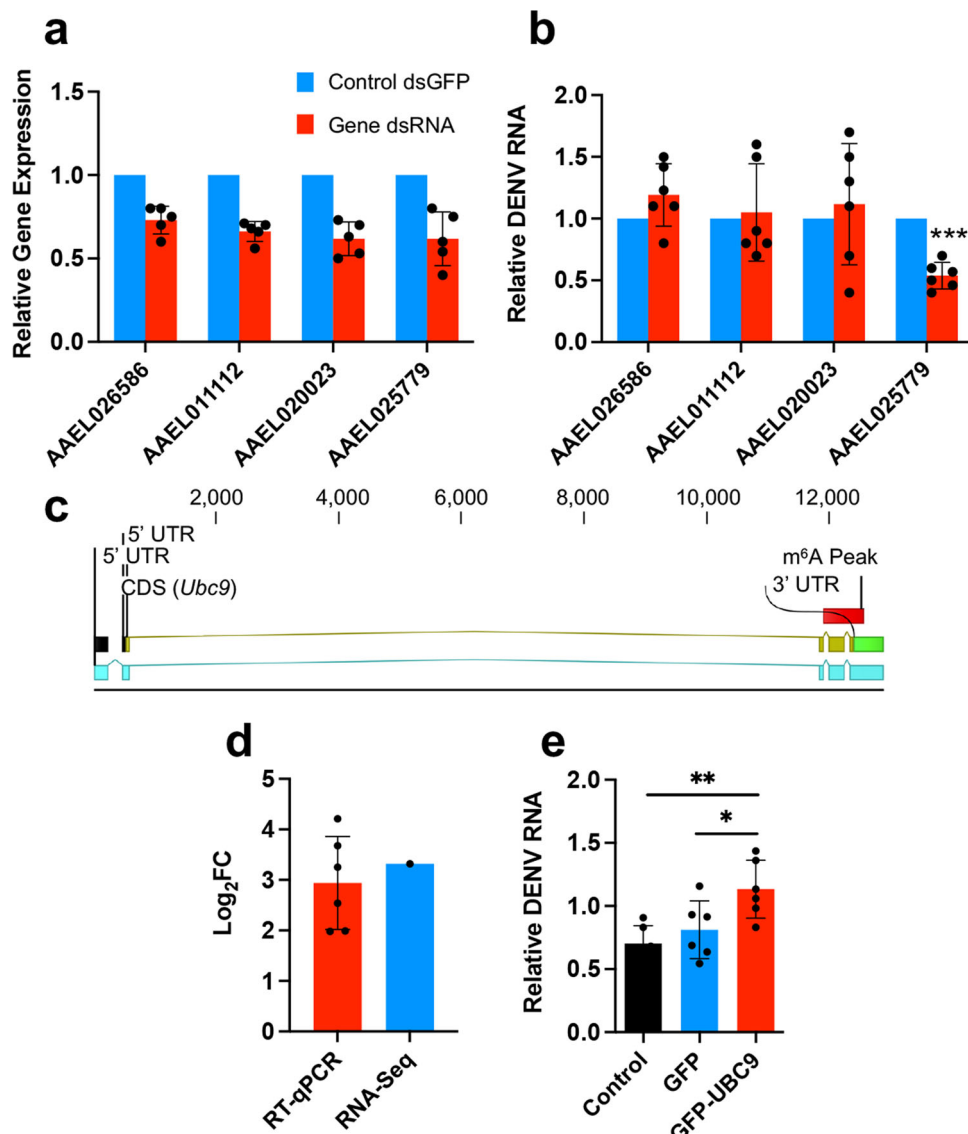
Fig. 7 *Ubc9* facilitates DENV replication in *Ae. aegypti* cells. a Confirmation of silencing of four genes selected from differentially expressed genes by RNAi in Aag2 cells. **b** Inhibition of DENV replication by *Ubc9* (AAEL025779) silencing. Aag2 cells transfected with dsRNA targeting *GFP* or dsRNA targeting the four genes were infected with DENV-2 72 h after transfection. Cells were collected at 72 hpi for quantification of DENV RNA by RT-qPCR. Control *GFP* expression levels in **a** and **b** were adjusted to 1. ***$p < 0.001$ (*t*-test). **c** Location of the m⁶A peak in *Ubc9*. **d** RT-qPCR analysis of RNA from Aag2 cells infected with DENV for 72 h showed consistency in up-regulation of *Ubc9* transcript levels with the RNA-Seq data. FC, fold change. **e** Aag2 cells transfected with pSLfa-GFP or pSLfa-GFP-Ubc9 were infected with DENV 72 h after transfection. Cells were collected at 72 hpi for RNA extraction and quantification of DENV genomic RNA by RT-qPCR. Error bars represent mean ± S.D. *$p < 0.05$; **$p < 0.01$. One-way ANOVA with post hoc comparisons.

Virus titration. Plaque assay was used to measure virus titre in media as described previously[44]. Briefly, Vero cells (4×10^4 in 50 µl medium) were seeded in a 96-well plate and incubated at 37 °C until 90–100% confluent. Then, collected medium containing virus was diluted to 10^0, 10^{-1}, 10^{-2}, 10^{-3} with medium, and added into wells. Plates were first incubated for 1 h with shaking at room temperature and then incubated for an additional hour at 37 °C. After that, medium was removed from each well and to each well 50 µl of a mixture of 50% CMC gel (3% carboxymethyl cellulose) + 50% medium with FBS (final concentration of 4%) was added. The plate was incubated at 37 °C for 72 h. The overlay was discarded, then cells were fixed by adding 50 µl of ice-cold 80% acetone in PBS at −20 °C for 20 min and then air-dried overnight. Five percent skim milk in PBST (1× phosphate-Buffered Saline, 0.1% Tween) was used to block the cells. Cells were incubated with the primary antibody against DENV-2 Envelope protein (human) in 1:1000 dilution in 0.1% skim milk in 1×PBST for 2 h at 37 °C. After that, the plate was washed three times with PBS containing 0.05% Tween 20. Subsequently, cells were incubated with a secondary IR Dye conjugated anti-human antibody (Sigma) with 1% skim milk in PBST (1:5000) at 37 °C for 1 h. The plate was washed three times with PBS containing 0.05% Tween 20 and dried for 0.5 h. Virus plaques were detected by LI-COR Biosciences Odyssey infrared Imaging System and application software.

Dot blot. Total RNA was isolated from Aag2 and Vero cells. RNAs of the *EGFP* gene were synthesized in vitro by T7 RNA polymerase. Samples were diluted to 100 ng/µl and spotted on a polyvinylidene fluoride membrane (PVDF, Roche, Indianapolis, IN, USA). The membrane was UV-cross-linked and air-dried. The membrane was then blocked in the blocking buffer (5% skim milk in PBST) for 2 h at room temperature, and incubated with an m⁶A monoclonal antibody (1:1000; Synaptic Systems) overnight at 4 °C. After three washes with wash buffer (5% skim milk in PBST) for 10 min each, the membrane was incubated with an anti-mouse secondary antibody conjugated with an IR Dye (1:5000; Sigma) for 60 min at room temperature. After three washes as above, signals were detected with LI-COR Biosciences Odyssey infrared Imaging System and application software.

MeRIP-Seq. MeRIP-Seq was carried out by combining and modifying approaches described previously[16,27]. Aag2 cells seeded in 6-wells plates were infected with DENV serotype 2 East Timor strain (DENV-2 ET300) (MOI 1). At 5 days post-infection, total RNA was extracted using QIAzol lysis reagent (QIAGEN) and treated with TURBO DNase I (Thermo Fisher). Total RNA was fragmented using the RNA Fragmentation Reagent (Thermo Fisher) for 15 min. MeRIP was performed using EpiMark N⁶-methyladenosine Enrichment kit (NEB). Twenty-five microlitres of
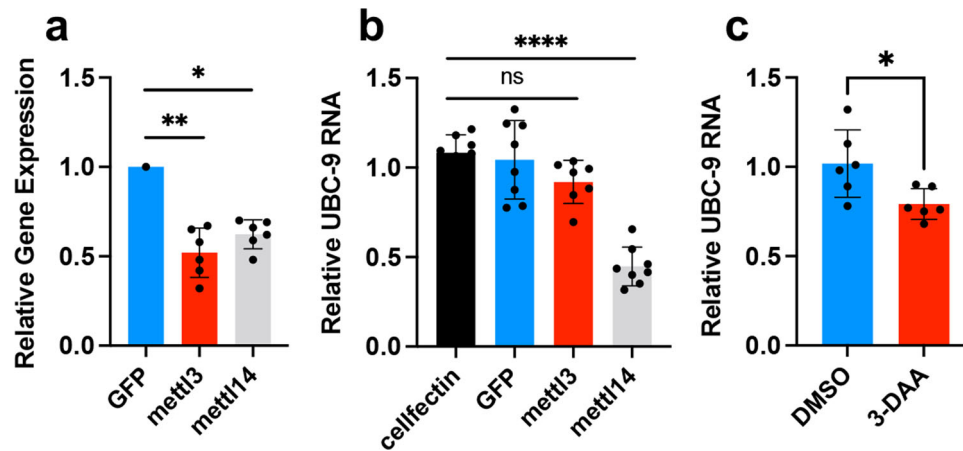
Fig. 8 Suppression of m⁶A modification reduces *Ubc9* transcript levels. a Confirmation of silencing of *METTL3* and *METTL14* by RNAi in Aag2 cells. Control GFP was adjusted to one. *$p < 0.05$; **$p < 0.01$ (one-way ANOVA with post hoc comparisons). **b** Decrease of *Ubc9* expression by silencing m⁶A writers. Aag2 cells were transfected with dsRNA targeting *GFP* or dsRNA targeting *METTL3* or *METTL14*. Cells were collected at 72 days post-transfection for quantification of *Ubc9* RNA levels by RT-qPCR. ****$p < 0.0001$; ns, not significant, one-way ANOVA with post hoc comparisons. **c** RT-qPCR was used to evaluate the transcript levels of *Ubc9* after using m⁶A inhibitor, 3-DAA. *$p < 0.05$ (t-test). Error bars represent mean ± S.D.
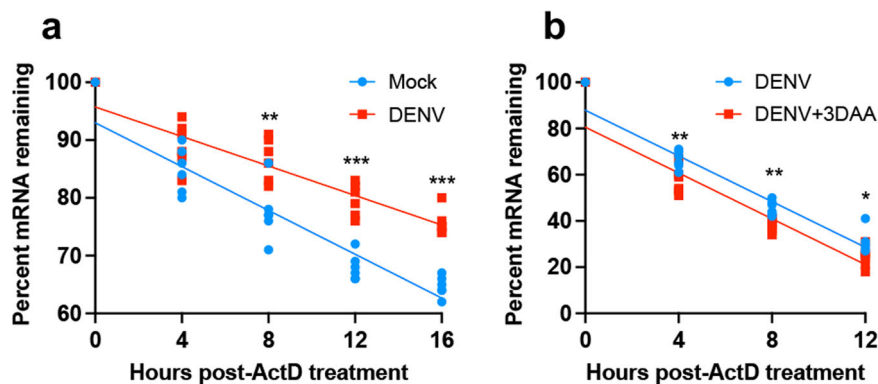

Fig. 9 DENV infection promotes *Ubc9* RNA stability. a Measurement of *Ubc9* RNA in mock and DENV-infected Aag2 cells. At 72 hpi, cell culture medium was replaced with medium containing 1 µM ActD. RNA was collected at the indicated times post-treatment and subjected to RT-qPCR to determine remaining relative RNA levels. **$p < 0.01$; ***$p < 0.001$ (t-test). **b** Measurement of *Ubc9* RNA in m⁶A DENV-infected m⁶A-inhibited Aag2 cells with 3-DAA. At 72 hpi, cell culture medium was replaced with medium containing 3-DAA. After 24 h post treatment, cell culture medium was replaced with medium containing ActD. RT-qPCR was used to measure the remaining relative RNA levels *$p < 0.05$; **$p < 0.01$ (t-test).

Protein G Dynabeads (Thermo Fisher) per sample was washed three times in MeRIP buffer (150 mM NaCl, 10 mM Tris-HCl [pH 7.5], 0.1% NP-40), and incubated with 1 µL anti-m⁶A antibody (Synaptic System) for 2 h at 4 °C with rotation. After washing three times with MeRIP buffer, anti-m⁶A conjugated beads were incubated with purified mRNAs with rotation at 4 °C overnight in 300 µL MeRIP buffer with 1 µL RNase inhibitor (recombinant RNasin; Promega). Ten percent of the mRNA sample was saved as the input fraction. Beads were then washed twice with 500 µL MeRIP buffer, twice with low salt wash buffer (50 mM NaCl, 10 mM Tris-HCl [pH 7.5], 0.1% NP-40), twice with high salt wash buffer (500 mM NaCl, 10 mM Tris-HCl [pH 7.5], 0.1% NP-40), and once again with MeRIP buffer. m⁶A-modified RNAs were eluted twice in 100 µL of MeRIP buffer containing 5 mM m⁶A salt (Santa Cruz Biotechnology) for 30 min at 4 °C with rotation. Eluates were pooled and concentrated by ethanol precipitation. RNA samples were submitted to Genewiz for RNA sequencing with Illumina Hiseq PE150. Three replicates were submitted per sample (IP and input), totalling 12 samples.

RNA-Seq data analysis. The CLC Genomics Workbench version 20.0.4 was used for bioinformatics analyses in this study. All input and m⁶A immunoprecipitated RNA (IP) libraries were trimmed from sequencing primers, adaptor sequences and low-quality reads. Low-quality reads (quality score below 0.05) and reads with more than two ambiguous nucleotides were discarded. Clean reads were aligned to the latest version of the *Ae. aegypti* reference genome (GCA_002204515.1) with mismatch, insertion, and deletion cost of 2, 3, and 3, respectively. Mapping was performed with stringent criteria and allowed a length fraction of 0.8 in mapping parameter, which encounter at least 80% of nucleotides in a read must be aligned to the reference genome. The minimum similarity between the aligned region of the read and the reference sequence was set at 80%.

The peak calling process was conducted by using CLC Epigenomics toolbox to identify the enriched regions of m⁶A peaks by comparing reads from the IP and input samples. As the first step of quality control, the input data was examined to check if the data satisfy the assumptions made by the algorithm and to compute several quality measures such as relative strand correlation and normalized strand coefficient[45–47]. After passing the quality control, estimated fragment length and estimated window size were calculated for peak calling process[48]. The CLC shape-based peak caller uses the characteristic of peak shape and enriched read coverage to identify peaks in MeRIP-seq data. The peak shape filter was applied to the experimental data and a score and the p-value were calculated at each genomic position. The score was obtained by extracting the genomic coverage profile of a window centred at the genomic position and then comparing this profile to the peak shape filter. The result of this comparison was defined as peak shape score by CLC Genomic Workbench. Once the peak shape score for the complete genome was calculated, peaks were identified as genomic regions where the maximum peak shape score was >1.28 and the p-value is smaller than the defined threshold (0.1). The centre of the peak was then identified as the genomic region with the highest peak shape score, and the boundaries were determined by the genomic positions where the peak shape score became negative[48]. The peak regions were extracted, and we searched for the presence of DRACH motif as methylation site within both strands of the peak regions. The peaks without DRACH motif enrichment were discarded. Peaks considered as true m⁶A peaks, if they were detected in at least two libraries with more than five associated reads in each individual IP samples and their normalised fold change in IP vs Input samples was greater than one (Fig. 1a). To define genes associated with the m⁶A peaks, the reference genome was annotated by the identified peaks and their relative positions data were exported if it overlapped with any annotated gene region. The peaks and the associated genes were then manually checked and any peaks within the gene region were retained for further downstream analysis.
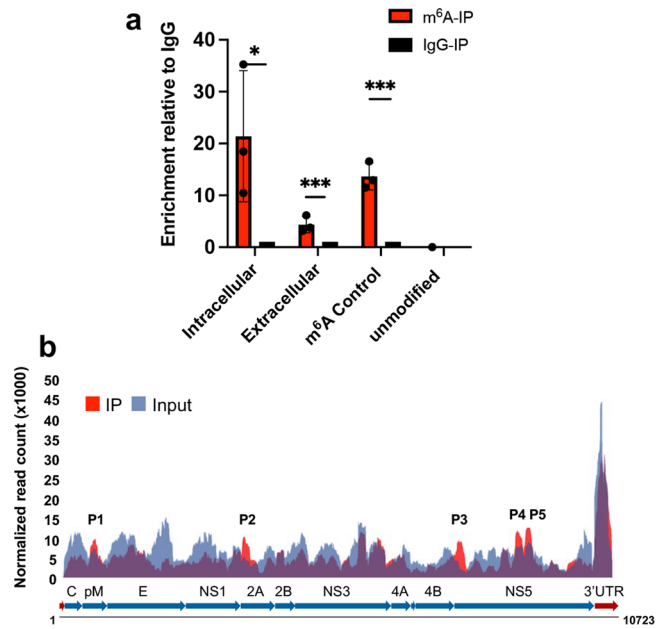
Fig. 10 DENV RNA is modified by m6A in infected mosquito cells.
a MeRIP-RT-qPCR analysis of RNA harvested from DENV-infected Aag2 cells (72 hpi) and immunoprecipitated with anti-m6A or IgG using primers to DENV genome. For the extracellular virions, the supernatant collected from DENV-infected cells was treated at room temperature with 17 µg of RNase A per ml for 20 min to remove any naked RNA. Eluted RNA was quantified as a percentage of input. m6A Control, positive control RNA with m6A modification; unmodified, negative control RNA without m6A modification. Error bars represent mean ± S.D. *$p \leq 0.01$, ***$p \leq 0.001$ (*t*-test). **b** Map of m6A-binding sites in the DENV RNA genome by MeRIP-Seq of RNA isolated from DENV-infected Aag2 cells based on three biological replicates. Read coverage, normalized to the total number of reads mapping to the viral genome for each experiment, is in red for MeRIP-Seq and in blue for input RNA-Seq. The five identified peaks (P1-P5) are indicated on the graph.

We performed the RNA-Seq analysis to identify the involvement of m6A sites in host dysregulated genes in response to DENV infection. We mapped the input reads to the *Ae. aegypti* reference genome and their expression profiles were produced by distributing and counting the reads across genes and transcripts. The relative expression levels were produced as RPKM (reads per kilobase of exon model per million mapped reads) values. We also used the same tools to identify altered m6A peaks in response to DENV infection. We used the normalised TPM (transcripts per million) value to compare m6A site modification in DENV-infected and non-infected samples. For both m6A peaks and DEGs, the total read counts were calculated based on average of total mappable reads from three replicate libraries.

The multi-factorial statistics based on a negative binomial generalized linear model (GLM) was used to generate differential expression profile. Each gene is modelled by a separate GLM and this approach allows us to fit curves to expression values without assuming that the error on the values is normally distributed. TMM (trimmed mean of M values) normalization method was applied to all datasets to calculate effective library sizes, which were then used as part of the per-sample normalization[49]. The Wald Test was also used to compare each sample against its control group to test whether a given coefficient is non-zero. We considered genes with more than 2-fold change and *p*-value of <0.05 as statistically significantly modulated genes.

All the *Ae. aegypti* genes with m6A peaks were uploaded on the Blast2GO[50] server for functional annotation and GO analysis. We used BLAST, InterProScan[51], enzyme classification codes (EC) and EggNOG[52] to determine the GO terms of the differentially expressed sequences. More abundant terms were computed for each category of molecular function, biological process, and cellular components. An enrichment analysis using Fisher's Exact Test was done using all AaegL5.0 annotated genes as the reference dataset by FatiGO package, which is integrated in Blast2GO. Overrepresented terms were considered if their enrichment fold change was >1.5 and the *p*-value was lower than 0.05. A bar chart was produced showing the *p*-values and fold changes for the top 20 most abundant GO terms among all enriched terms for each category of biological process, molecular function, and cellular components. We also use REVIGO[53] to visualize the semantic relationships in highly redundant list of GO terms. The identified GO terms and their *p*-value

were used as input in this tool. The GO terms have been clustered based on semantic similarity measure of SimRel and their frequenting calculated from whole UniProt database.

RT-qPCR and MeRIP-RT-qPCR. Total RNA was extracted from Aag2 cells and treated with DNase I using TURBO DNase (ThermoFisher Scientific). cDNA (2µg) was synthesised using SuperScript™ III Reverse Transcriptase (ThermoFisher Scientific) followed by qPCR using QuantiFast SYBR Green PCR mix (Qiagen) in accordance with the manufacturer's instructions. RT-qPCRs were carried out using a Rotor-Gene thermal cycler (QIAGEN). For qPCR, cDNA was diluted in 1:5 with UltraPure DNase/RNase-free water (Invitrogen). Two microlitres of the diluted cDNA was used in 10 µL qPCR reactions with both forward and reverse gene-specific primers (10 µM) with an initial 95 °C 5 min, and 40 cycles of 95 °C 20 s, 65 °C 15 s, 72 °C 10 s. Each reaction was run with at least three biological replicates, each with three technical replicates. The *RPS17* gene was used for normalizing data. Primer sequences are provided in Supplementary Table 2.

For MeRIP-RT-qPCR, EpiMark N6-Methyladenosine Enrichment Kit was first used to conduct MeRIP on total RNA harvested from DENV-infected Aag2 cells according to the manufacturer's instructions (New England BioLabs). This was followed by RT-qPCR as above. Positive and negative controls for m6A were provided in the kit.

RNAi-mediated gene silencing. For RNAi experiments, dsRNAs were synthesized in vitro using the T7 MEGAscript transcription kit according to the manufacturer's instructions (ThermoFisher Scientific, USA). T7 promoter sequences were incorporated in both forward and reverse primers (Supplementary Table 2). For dsRNA synthesis, 200–500 ng of PCR product was used for each reaction. The reaction was incubated at 37 °C overnight, DNase-treated, and precipitated by the lithium chloride method following the manufacturer's instructions. Four micrograms of the dsRNA was used to transfect Aag2 cells with 5 µl of Cellfectin transfection reagent (Invitrogen, USA). The cells were transfected again with the same reagent at 72 h after the first transfection. Cells were collected for RNA extraction as required for further analysis at 48 h after the second transfection.

Treatment of cells with 3-DAA. The methylation inhibitor 3-Deazaadenosine (3-DAA; D8296, Sigma-Aldrich) was used to inhibit RNA methylation[54]. Aag2 cells were treated with 100 µM 3-DAA or as indicated in the text. Cells were collected for mRNA analysis at 48 h post-treatment.

Measurement of RNA stability. Aag2 cells were plated in 12-well plates and then infected with DENV-2 at MOI 1. At 3 days post-infection, medium was changed to the 1:1 Mitsuhashi-Maramorosch and Schneider's insect medium which contained 1 µM Actinomycin D (Sigma-Aldrich). After 4, 8, 12 and 16 h post-treatment, total RNA was extracted from the Aag2 cells using QIAzol lysis reagent (QIAGEN) and treated with TURBO DNase I (Thermo Fisher). The percent of *Ubc9* mRNA remaining was analysed through RT-qPCR.

Overexpression of Ubc9 protein. The complete open reading frame for *Ubc9* was cloned downstream of the *GFP* gene in the plasmid vector pSLfa-PUb (Addgene) under the polyubiquitin promoter. For overexpression, 2 µg of the plasmid was transfected into Aag2 cells using the Cellfectin reagent (Invitrogen) according to the manufacturer's instructions.

Statistics and reproducibility. For all the statistical analyses and production of the graphs GraphPad Prism version 9 was used. Data were tested for normality using Shapiro–Wilk test. *T*-test was used to determine the significance levels between two samples, and One-way ANOVA was used to determine significance levels between three or more treatments. More details, including the number of replicates, are provided in the relevant figure legends. Data points on graphs represent *n* = biological replicates.

Reporting summary. Further information on research design is available in the Nature Research Reporting Summary linked to this article.

Data availability
MeRIP-Seq data have been deposited in the SRA under the accession PRJNA668808.

References
1. Boccaletto, P. et al. MODOMICS: a database of RNA modification pathways. 2017 update. *Nucleic Acids Res.* **46**, D303–d307 (2018).

2. Cao, G., Li, H. B., Yin, Z. & Flavell, R. A. Recent advances in dynamic m6A RNA modification. *Open Biol.* **6**, 160003 (2016).

3. Lence, T. et al. m6A modulates neuronal functions and sex determination in *Drosophila*. *Nature* **540**, 242–247 (2016).

4. Park, C. H. & Hong, K. Epitranscriptome: m6A and its function in stem cell biology. *Genes Genomics* **39**, 371–378 (2017).

5. Tong, J., Flavell, R. A. & Li, H. B. RNA m6A modification and its function in diseases. *Front. Med.* **12**, 481–489 (2018).

6. Williams, G. D., Gokhale, N. S. & Horner, S. M. Regulation of viral infection by the RNA modification N6-methyladenosine. *Annu. Rev. Virol.* **6**, 235–253 (2019).

7. Wang, X. et al. Structural basis of N6-adenosine methylation by the METTL3-METTL14 complex. *Nature* **534**, 575–278 (2016).

8. Csepany, T., Lin, A., Baldick, C. J. & Beemon, K. Sequence specificity of mRNA N6-adenosine methyltransferase. *J. Biol. Chem.* **265**, 20117–20122 (1990).

9. Fu, Y., Dominissini, D., Rechavi, G. & He, C. Gene expression regulation mediated through reversible m6A RNA methylation. *Nat. Rev. Genet.* **15**, 293–306 (2014).

10. Ke, S. et al. A majority of m6A residues are in the last exons, allowing the potential for 3′ UTR regulation. *Genes Dev.* **29**, 2037–2053 (2015).

11. Jia, G. et al. N6-methyladenosine in nuclear RNA is a major substrate of the obesity-associated FTO. *Nat. Chem. Biol.* **7**, 885–887 (2011).

12. Zheng, G. et al. ALKBH5 is a mammalian RNA demethylase that impacts RNA metabolism and mouse fertility. *Mol. Cell* **49**, 18–29 (2013).

13. Wang, X. et al. N6-methyladenosine modulates messenger RNA translation efficiency. *Cell* **161**, 1388–1399 (2015).

14. Wang, Y. et al. N6-methyladenosine modification destabilizes developmental regulators in embryonic stem cells. *Nat. Cell Biol.* **16**, 191–198 (2014).

15. HsuChen, C. C. & Dubin, D. T. Methylated constituents of *Aedes albopictus* poly (A)-containing messenger RNA. *Nucleic Acids Res.* **4**, 2671–2682 (1977).

16. Li, B. et al. Transcriptome-wide analysis of N6-methyladenosine uncovers its regulatory role in gene expression in the lepidopteran *Bombyx mori*. *Insect. Mol. Biol.* **28**, 703–715 (2019).

17. Rodenhuis-Zybert, I. A., Wilschut, J. & Smit, J. M. Dengue virus life cycle: viral and host factors modulating infectivity. *Cell Mol. Life Sci.* **67**, 2773–2786 (2010).

18. Bhatt, S. et al. The global distribution and burden of dengue. *Nature* **496**, 504–507 (2013).

19. Gubler, D. J. The continuing spread of West Nile virus in the western hemisphere. *Clin. Infect. Dis.* **45**, 1039–1046 (2007).

20. St. John, A. L. Influence of mast cells on dengue protective immunity and immune pathology. *PLoS Pathog.* **9**, e1003783 (2013).

21. Vervaeke, P., Vermeire, K. & Liekens, S. Endothelial dysfunction in dengue virus pathology: Endothelial dysfunction in dengue virus pathology. *Rev. Med. Virol.* **25**, 50–67 (2015).

22. Gokhale, N. S. et al. N6-methyladenosine in *Flaviviridae* viral RNA genomes regulates infection. *Cell Host Microbe* **20**, 654–665 (2016).

23. Lichinchi, G. et al. Dynamics of human and viral RNA methylation during Zika virus infection. *Cell Host Microbe* **20**, 666–673 (2016).

24. Chen, X.-Y., Zhang, J. & Zhu, J.-S. The role of m6A RNA methylation in human cancer. *Mol. Cancer* **18**, 103 (2019).

25. Liu, H. et al. Accurate detection of m6A RNA modifications in native RNA sequences. *Nat. Commun.* **10**, 4079 (2019).

26. McIntyre, W. et al. Positive-sense RNA viruses reveal the complexity and dynamics of the cellular and viral epitranscriptomes during infection. *Nucleic Acids Res.* **46**, 5776–5791 (2018).

27. Gokhale, N. S. et al. Altered m6A modification of specific cellular transcripts affects *Flaviviridae* infection. *Mol. Cell* **77**, 542–555.e548 (2020).

28. Castillo-Méndez, M. & Valverde-Garduño, V. *Aedes aegypti* immune response and its potential impact on dengue virus transmission. *Viral Immunol.* **33**, 38–47 (2020).

29. Serrato-Salas, J. et al. *Aedes aegypti* antiviral adaptive response against DENV-2. *Dev. Comp. Immunol.* **84**, 28–36 (2018).

30. Villordo, S. M., Filomatori, C. V., Sánchez-Vargas, I., Blair, C. D. & Gamarnik, A. V. Dengue virus RNA structure specialization facilitates host adaptation. *PLoS Pathog.* **11**, e1004604 (2015).

31. de Borba, L. et al. RNA structure duplication in the dengue virus 3′ UTR: redundancy or host specificity? *mBio* **10**, e02506–e02518 (2019).

32. Bentz, G. L., Moss, C. R., Whitehurst, C. B., Moody, C. A. & Pagano, J. S. LMP1-induced sumoylation influences the maintenance of Epstein-Barr virus latency through KAP1. *J. Virol.* **89**, 7465–7477 (2015).

33. Volcic, M. et al. Vpu modulates DNA repair to suppress innate sensing and hyper-integration of HIV-1. *Nat. Microbiol.* **5**, 1247–1261 (2020).

34. Wang, C. et al. HA triggers the switch from MEK1 SUMOylation to phosphorylation of the ERK pathway in Influenza A virus-infected cells and facilitates its infection. *Front. Cell Infect. Microbiol.* **7**, 27 (2017).

35. Wilson, V. G. Introduction to SUMOylation. *Adv. Exp. Med. Biol.* **963**, 1–12 (2017).

36. Hay, R. T. SUMO: a history of modification. *Mol. Cell* **18**, 1–12 (2005).

37. Domingues, P. et al. Global reprogramming of host SUMOylation during Influenza virus infection. *Cell Rep.* **13**, 1467–1480 (2015).

38. Bohl, C. R., Abrahamyan, L. G. & Wood, C. Human Ubc9 is involved in intracellular HIV-1 Env stability after trafficking out of the trans-Golgi network in a Gag dependent manner. *PLoS ONE* **8**, e69359 (2013).

39. Chiu, M.-W., Shih, H.-M., Yang, T.-H. & Yang, Y.-L. The type 2 dengue virus envelope protein interacts with small ubiquitin-like modifier-1 (SUMO-1) conjugating enzyme 9 (Ubc9). *J. Biomed. Sci.* **14**, 429–444 (2007).

40. Su, C.-I., Tseng, C.-H., Yu, C.-Y. & Lai, M. M. C. SUMO modification stabilizes dengue virus nonstructural protein 5 to support virus replication. *J. Virol.* **90**, 4308–4319 (2016).

41. Stokes, S. et al. The SUMOylation pathway suppresses arbovirus replication in *Aedes aegypti* cells. *PLoS Pathog.* **16**, e1009134 (2020).

42. Du, Y. et al. SUMOylation of the m6A-RNA methyltransferase METTL3 modulates its function. *Nucleic Acids Res.* **46**, 5195–5208 (2018).

43. Xu, H. et al. SUMO1 modification of methyltransferase-like 3 promotes tumor progression via regulating Snail mRNA homeostasis in hepatocellular carcinoma. *Theranostics* **10**, 5671–5686 (2020).

44. Zhang, G., Asad, S., Khromykh, A. A. & Asgari, S. Cell fusing agent virus and dengue virus mutually interact in *Aedes aegypti* cell lines. *Sci. Rep.* **7**, 6935 (2017).

45. Landt, S. G. et al. ChIP-seq guidelines and practices of the ENCODE and modENCODE consortia. *Genome Res.* **22**, 1813–1831 (2012).

46. Kumar, V. et al. Uniform, optimal signal processing of mapped deep-sequencing data. *Nat. Biotech.* **31**, 615–622 (2013).

47. Marinov, G. K., Kundaje, A., Park, P. J. & Wold, B. J. Large-scale quality analysis of published ChIP-seq data. *G3* **4**, 209–223 (2014).

48. Strino, F. & Lappe, M. Identifying peaks in *-seq data using shape information. *BMC Bioinform.* **17**, 206 (2016).

49. Robinson, M. & Oshlack, A. A scaling normalization method for differential expression analysis of RNA-seq data. *Genome Biol.* **11**, R25 (2010).

50. Götz, S. et al. High-throughput functional annotation and data mining with the Blast2GO suite. *Nucleic Acids Res.* **36**, 3420–3435 (2008).

51. Jones, P. et al. InterProScan 5: genome-scale protein function classification. *Bioinformatics* **30**, 1236–1240 (2014).

52. Huerta-Cepas, J. et al. eggNOG 5.0: a hierarchical, functionally and phylogenetically annotated orthology resource based on 5090 organisms and 2502 viruses. *Nucleic Acids Res.* **47**, D309–D314 (2019).

53. Supek, F., Bošnjak, M., Škunca, N. & Šmuc, T. REVIGO summarizes and visualizes long lists of gene ontology terms. *PLoS ONE* **6**, e21800 (2011).

54. Fustin, J.-M. et al. RNA-methylation-dependent RNA processing controls the speed of the circadian clock. *Cell* **155**, 793–806 (2013).

Acknowledgements

Author contributions

S.A. and Z.D. designed the project. Z.D. conducted all the experiments. K.E. analysed the MeRIP-Seq data. Z.D. wrote the first draft. All authors contributed to the writing and editing of the manuscript.

Competing interests

The authors declare no competing interests.

Additional information

Supplementary information The online version contains supplementary material available at https://doi.org/10.1038/s42003-022-03566-8.

Correspondence and requests for materials should be addressed to Sassan Asgari.

Peer review information *Communications Biology* thanks Qingfeng Zhang and the other anonymous reviewers for their contribution to the peer review of this work. Primary Handling Editor: Gene Chong.

Reprints and permission information is available at http://www.nature.com/reprints

Publisher's note Springer Nature remains neutral with regard to jurisdictional claims in published maps and institutional affiliations.